Successive Use of Amphiphilic Block Copolymers as Nanoreactors and Templates: Preparation of Porous Silica with Metal Nanoparticles

Lyudmila Bronstein,*,† Eckhard Krämer,‡ Beate Berton,‡ Christian Burger,‡ Stephan Förster,‡ and Markus Antonietti‡

Nesmeyanov Institute of Organoelement Compounds, Russian Academy of Sciences, 28 Vavilov Street, Moscow 117813, Russia, and Max Planck Institut of Colloids and Interfaces, Kantstrasse 55, D-14513 Teltow-Seehof, Germany

Received November 5, 1998
Revised Manuscript Received March 8, 1999

Amphiphilic block copolymers (ABCs) offer many new synthetic options to form mesostructured materials which have been well-described in a large number of papers and several comprehensive reviews.[1−4] In particular, they can be employed as nanoreactors for both metal and semiconductor particle formation, both in selective solvents and in bulk, if at least one of the blocks is designed to interact with metal salts and metals.[5−8]

On the other hand, several types of amphiphilic block copolymers which form micelles in water can be used as templates to prepare mesoporous silicates[9−12] or other types of microporous materials,[13] for which synthesis was performed with surfactants for several years.[14,15] Here we extend the use of ABCs as synthetic templates.

In this paper, we combine both approaches and use special block copolymers, polybutadiene-*b*-poly(ethylene oxide)s (PB-*b*-PEO), in a first step as nanoreactors for preparation of metal nanoparticles inside their micelle cores and then as templates where the micelles are used as porogens. The final product after calcination of the polymer is silica with discrete nanoparticles located on the pore walls as presented in Chart 1.

Chart 1

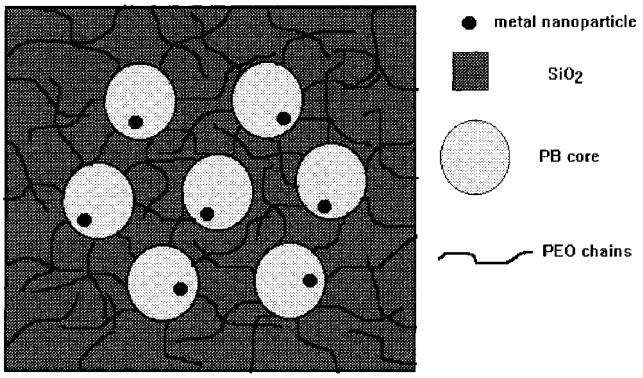

Table 1. Characteristics of the PB-*b*-PEO Block Copolymers

notation	M_{PB}	M_{PEO}	M_w/M_n
PB-*b*-PEO-I	13400	19200	1.06
PB-*b*-PEO-II	1070	5290	1.05
PB-*b*-PEO-III	6160	6200	1.02

We describe the interaction of the double bonds of PB with different Pd and Pt compounds, metal colloid formation, and several routes for the preparation of microporous silicates with metal nanoparticles.

Table 1 shows the characteristics of three different samples of PB-*b*-PEO block copolymers synthesized by anionic polymerization.[16]

These three different polymers were chosen because they show different aggregate morphologies and cover a wide molecular weight range, which gives different sizes of both nanoparticles and pores.

The very asymmetric PB-*b*-PEO-II with its rather short PB block forms spherical micelles in aqueous solution with a hydrodynamic diameter of $D_h = 24.5$ nm, as determined by dynamic light scattering. The slightly asymmetric PB-*b*-PEO-I, possessing a comparably high molecular weight, shows under standard conditions a coexistence of spherical micelles (D = 49 nm) and wormlike micelles with a cross section of 32 nm. The symmetric sample PB-*b*-PEO-III exclusively forms wormlike micelles with a cross section of 17 nm, which mutually interact and form networks. The latter two aggregation morphologies were characterized by electron microscopy and will be illustrated below. We stress that the cylindrical micelles and their networks decorated with metal nanoparticles result in cylindrical channels with functionalized walls that can be promising for various applications.

As metal salts for micelle loading, $(CH_3CN)_2PdCl_2$, the Zeise salt ($KPt(C_2H_4)Cl_3$), and K_2PtCl_4 were purchased from Aldrich and used as received. Earlier work on the synthesis of Pd-, Pt-, and Rh-containing polymers derived from block copolymers with the PB-1,2 block in organic media showed that the metal salts bind the

* To whom correspondence should be addressed.
† Russian Academy of Sciences.
‡ Max Planck Institute of Colloids and Interfaces.

(1) Forster, S.; Antonietti, M. *Adv. Mater.* **1998**, *10* (3), 195.
(2) Tuzar, Z.; Kratochvil, P. In *Surface and Colloid Science*; Matijevic, E., Ed.; Plenum Press: New York, 1993; Vol. 15.
(3) Desjardins, A.; Van de Ven, T. G. M.; Eisenberg, A. *Macromolecules* **1992**, *25*, 2412.
(4) Zhang, L.; Yu, K.; Eisenberg, A. *Science* **1996**, *272*, 1777.
(5) Chan, Y. N. C.; Schrock, R. R.; Cohen, R. E. *Chem. Mater.* **1992**, *4*, 24.
(6) Antonietti, M.; Wenz, E.; Bronstein, L. M.; Seregina, M. V. *Adv. Mater.* **1995**, *7*, 1000.
(7) Spatz, J. P.; Roescher, A.; Möller, M. *Adv. Mater.* **1996**, *8*, 337.
(8) Moffit, M.; Eisenberg, A. *Chem. Mater.* **1995**, *7*, 1178.
(9) Antonietti, M.; Goltner, C. *Angew. Chem.* **1997**, *109*, 944.
(10) Zhao, D.; Feng, J.; Huo, Q.; Melosh, N.; Fredrikson, G. F.; Chmelka, B. F.; Stucky, G. D. *Science* **1998**, *279*, 548.
(11) Goltner, C.; Henke, S.; Weissenberger, M. C.; Antonietti, M. *Angew. Chem.* **1998**, *37*, 613.
(12) (a) Krämer, E.; Förster, S.; Göltner, C.; Antonietti, M. *Langmuir* **1998**, *14*, 2027, (b) Göltner, C.; Berton, B.; Krämer, E.; Antonietti, M. *Chem. Commun.*, accepted
(13) Templin, M.; Frank, A.; Chesne, A. D.; Leist, H.; Zhang, Y.; Ulrich, R.; Schadler, V.; Wiesner, U. *Science* **1997**, *278*, 1795.
(14) (a) Kresge, C. T.; Leonowicz, M. E.; Roth, W. J.; Vartuli, J. C.; Beck, J. S. *Nature* **1992**, *359*, 710. (b) Tanev, P. T.; Pinnavaia, T. J. *Science* **1996**, *271*, 1267.
(15) (a) Burkett, S. L.; Sims, S. D.; Mann, S. *Chem. Commun.* **1996**, 1367. (b) Fowler, C. E.; Burkett, S. L.; Mann, S. *Chem. Commun.* **1997**, 1769.
(16) Förster, S.; Krämer, E., to be published.

10.1021/cm980762h CCC: $18.00 © 1999 American Chemical Society
Published on Web 05/13/1999

olefin groups via π complexes.[17,18] Here we have found that similar complexes are obtained for the present case in water as a solvent. The reaction between $(CH_3CN)_2PdCl_2$, or the Zeise salt (or K_2PtCl_4), and PB-*b*-PEO was performed in aqueous solution at room temperature and a molar ratio of PB:Mt = 4:1. While there are evidences that a PEO block behaving like a crown ether in an organic medium can coordinate with selected metal compounds (for instance, with $LiAuCl_4$),[19] the behavior of the PEO block in water is completely different. Though some interaction of $CaCl_2$ and NaCl with PEO chains in water, which changed the morphology of block copolymers, was described in ref 20, the real coordination of noble metal compounds with oxygen of PEO units was not observed. Moreover, in ref 21 we have clearly shown that in the case of poly(ethyleneimine)-*block*-poly(ethylene oxide) (PEI-*b*-PEO), only PEI units interact with Pd and Pt compounds in water, which results in micelle formation. For PB-*b*-PEO block copolymers, we conclude that the interaction with metal compounds proceeds solely in the PB block.

Because the reaction products formed during the complexation (CH_3CN or KCl) stay in the reaction solution, an equilibrium is maintained where a part of the Pd or Pt compounds remains nonreacted outside of micelles. However, solely micellar-bound metal π-olefin complexes were obtained by removal of the side products by 3-fold ultrafiltration of the reaction solution using an Amicon ultrafiltration system, employing concentration cycles of up to 20 wt % polymer followed by dilution of the concentrated solution with pure water. As a result, the last washing water was clean (confirming the lack of metal compound), while the micellar solution was dark brown (Pd) or yellow (Pt).

Reduction of Pd or Pt species was carried out with H_2 by bubbling through the solution at room temperature for 10 min. The fact that a micellar-bound Pt species gives a much better control of both particle size and distribution is underlined by comparing the transmission electron micrographs (TEMs) of Pt colloids prepared via H_2 reduction of the initial reaction solution (Figure 1a) and those of the purified, ultrafiltrated one (Figure 1b).

In Figure 1a one can see that both spherical and wormlike micelles are decorated with tiny Pt particles having a mean diameter less than 2 nm. At the same time, the sample contains big, irregular particle aggregates (17−27 nm in size) which are composed of small Pt particles obviously nucleated in a continuous phase and not sufficiently stabilized by block copolymer. In contrast, the ultrafiltrated solutions produce nanoparticles located solely in block copolymer micelles (Figure 1b). This is a favorable position for the metal nanoparticles from the viewpoint of templating, because such metal nanoparticles will become located outside

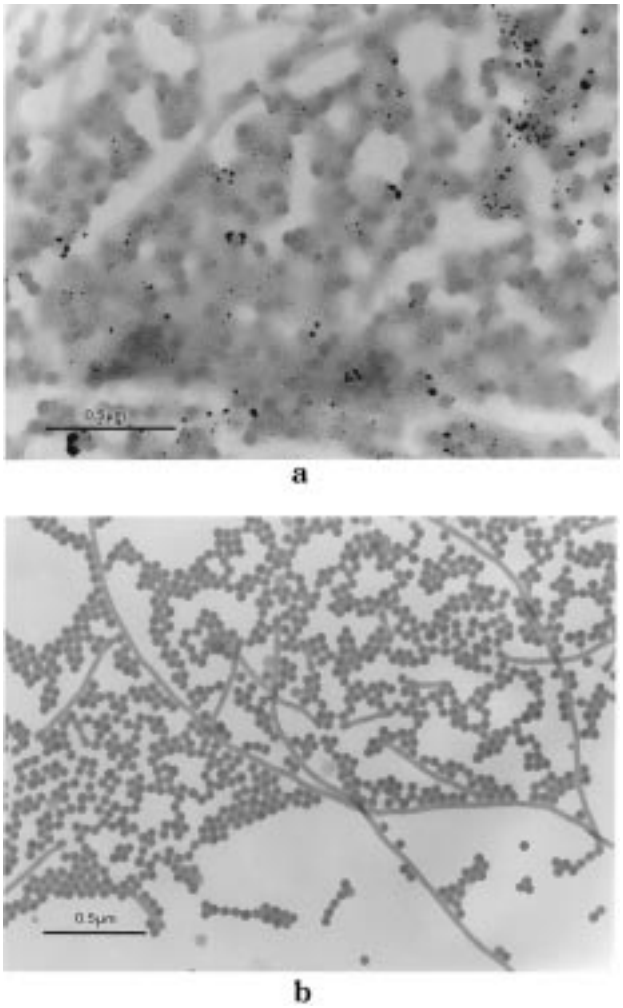

Figure 1. TEMs of the Pt colloids prepared in PB-*b*-PEO-I without ultrafiltration (a) and after ultrafiltration (b).

of the silica network. A similar purification effect was also obtained for the Pd-loaded samples.

The typical templating procedure was as follows: the metal nanoparticle/PB-*b*-PEO micellar solution was ultrafiltrated to about 20−25 wt %, and tetramethoxysilane (TMOS) was added (4 g of TMOS/2 g of H_2O). The exposure to gaseous HCl for several seconds initiated hydrolysis. The methanol produced in the reaction was removed using a rotary evaporator finally at 30 mbar vacuum at 40 °C. Then the sample was kept at 50 °C for 20 h to allow condensation to be complete. Removal of organic materials from the silicas was carried out in a quartz tube at 500 °C for 4 h under nitrogen, followed by 12 h under oxygen. The completeness of removal was confirmed by thermogravimetric analysis. The molar ratios of TMOS/PEO varied from 3.7:1 for PB-*b*-PEO-II, to 5:1 for PB-*b*-PEO-I, and to 7:1 for PB-*b*-PEO-III, which provided stability of resulting silica in all of the cases.

Casting the silica from the ultrafiltrated, Pd nanoparticle containing the PB-*b*-PEO-I (MS−Pd-1) sample, we observe that the structure of the microporous material (Figure 2b) practically completely reproduces the structure of the template (Figure 2a). Indeed, a TEM of MS−Pd-1 contains spherically shaped pores with a diameter of about 39 nm and cylindrical pores with a cross section of 26 nm. The quantitative comparison

(17) Bronstein, L. M.; Seregina, M. V.; Platonova, O. A.; Kabachii, Yu. A.; Chernyshov, D. M.; Ezernitskaya, M. G.; Dubrovina, L. V.; Bragina, T. P.; Valetsky, P. M. *Makromol. Chem.* **1998**, *199*, 1357.
(18) Bronstein, L.; Seregina, M.; Valetsky, P.; Breiner, U.; Abetz, V.; Stadler, R. *Polym. Bull.* **1997**, *39*, 361.
(19) Roescher, A.; Möller, M. *Proc. ACS Meeting, PMSE Div.* **1995**, *73*, 156.
(20) Desjardins, A.; Van de Ven, T. G. M.; Eisenberg, A. *Macromolecules* **1992**, *25*, 2412.
(21) Bronstein, L. M.; Sidorov, S. N.; Gourkova, A. Y.; Valetsky, P. M.; Hartmann, J.; Breulmann, M.; Cölfen, H.; Antonietti, M. *Inorg. Chim. Acta* **1998**, *280*, 348.

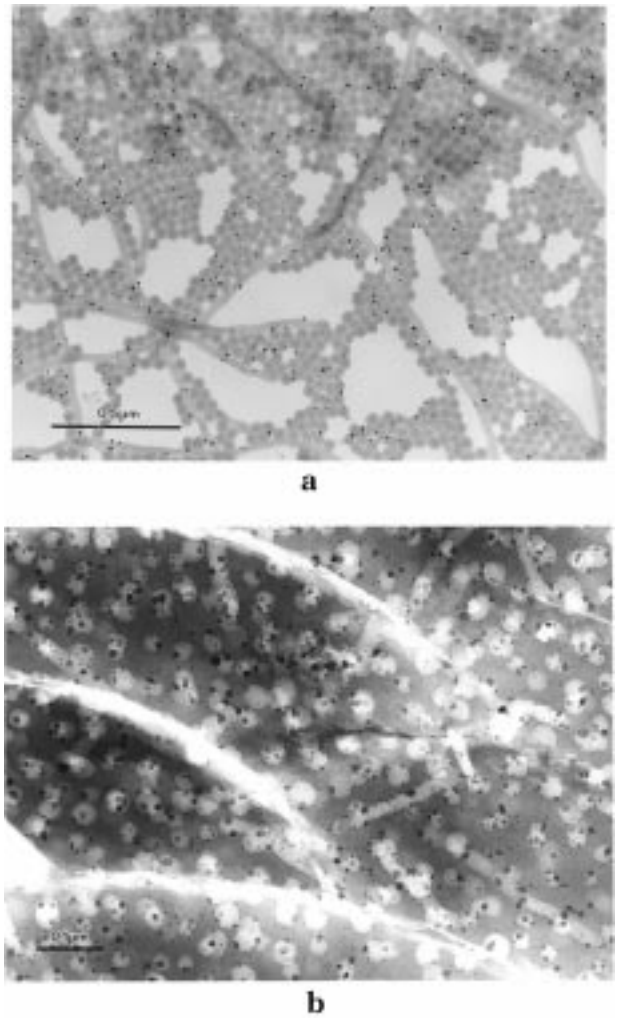

Figure 2. TEMs of the Pd colloids formed in the PB-*b*-PEO-I block copolymer micelles (a) and microporous silica obtained from PB-*b*-PEO-I−Pd(0) as the template after calcination (b).

between template and pore size seems to indicate a slight shrinkage during calcination. One can see that metal nanoparticles are mainly located in pores formed by the template, while smaller particles penetrate into smaller pores, presumably formed during calcination while burning off the PEO chains.

To estimate mean metal nanoparticle size and type, wide-angle X-ray scattering (WAXS) analysis was employed. For correct calculation of the particle size, several procedures were used: fitting of the peaks to a suitable peak shape profile (Cauchy functions fit well) plus background on a scattering vector scale and extracting the integral widths from these fits. This evaluation shows that the Pd nanoparticles (broad Bragg peaks, less than 4 nm diameter) convert during oxidative calcination at 500 °C into PdO particles of 5 nm size. For the employment of such materials as catalysts in various organic reactions, the formation of zero-valence Pd particles is necessary. This can be performed by treating the microporous silica MS−Pd-1 in ethanol with H_2 at 40 °C. Within 10 min the powder turned from brown to black. WAXS measurements performed after 1 h of the H_2 treatment revealed that the sample contained pure Pd(0) nanoparticles of the same diameter. By elemental analysis, MS−Pd-1 contained 1.96 wt % Pd.

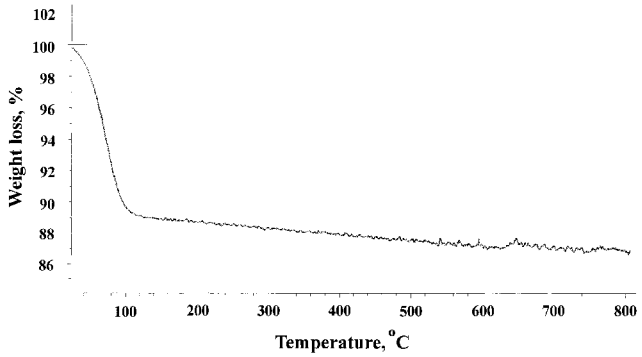

Figure 3. TGA plot of the MS−Pd-1a sample recorded in oxygen.

Thermogravimetric analysis (TGA) of MS−Pd-1a in oxygen, which was performed up to 800 °C, displays only about 1% weight loss other than the release of adsorbed H_2O observed at about 100 °C (Figure 3). These data affirm the completeness of calcination (removal of the organic part).

The use of the smaller PB-*b*-PEO-II as a template for casting of metal-containing microporous silica reveals some important peculiarities. The interaction of this block copolymer with Pd and Pt compounds proceeds in a manner similar to that of PB-*b*-PEO-II, but hydrogen reduction of such a sample in solution results in large nanoparticles. This is an indication that the growth of the particles is less well controlled by the low molecular weight block and the related loose micelle architecture. Because templating with PB-*b*-PEO-II results in a rather interesting fine pore diameter of 4 nm, it was relevant to find a way to suppress particle growth during reduction.

To accomplish that, the silica casting was performed prior to the metal nanoparticle generation; i.e., we first formed the silicic network around the PB-*b*-PEO-II micelles including the metal precursor, which is reduced in the second step. In this situation, the diameter of the metal nanoparticle did not have to exceed the pore size. Thus, we have loaded PB-*b*-PEO-II with $(CH_3CN)_2PdCl_2$, casted the silica (sample code MS−Pd-2), and reduced the compound before calcination in a H_2 atmosphere at 50 °C overnight. According to WAXS, very small particles were formed, the diameter of which was below the limit of the numerical analysis. The TEM of MS−Pd-2a after calcination (Figure 4) exhibits the typical channel system of mesoporous silica with embedded PdO particles.

With WAXS, the particle size after calcination was determined to be $d = 8.6$ nm, so the particles grow even larger than might be expected judging by the pore size. As seen before, PdO can be reduced to elementary Pd, and TGA of MS−Pd-2a reveals only a 1 wt % loss up to 800 °C. The sample contained 1.72 wt % Pd. To our disappointment, direct conversion of the precursor metal compound during oxidative calcination (i.e., without intermediate reduction) resulted in rather big, unstructured PdO particles being larger than the pores, most of them held at grain boundaries or located outside of the pore channel system. For this case, it is assumed that the Pd intermediates or small Pd clusters are expelled from the channel system together with the volatile organic decomposition products. Thus, a block

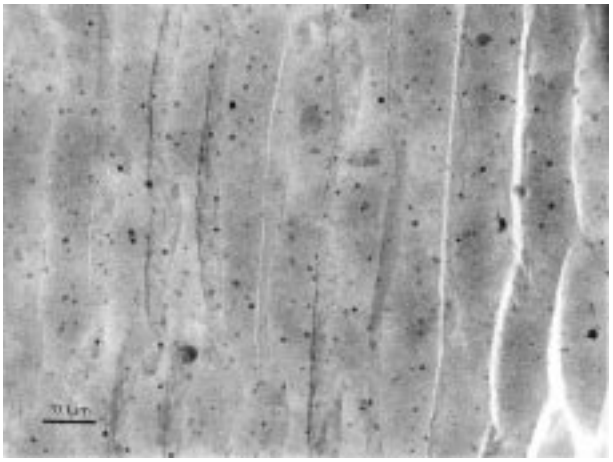

Figure 4. TEM of MS−Pd-2a after calcination (derived from PB-*b*-PEO-II).

copolymer with a very short core block used as a template does not provide the intended location of nanoparticles inside the silica pores and does not control a particle size.

The morphology of the symmetric PB-*b*-PEO-III aggregates again differs from those of the two other samples. PB-*b*-PEO-III forms wormlike micelles, which even gel and precipitate in dilute solution (1 g/L) after interaction with $(CH_3CN)_2PdCl_2$. This can be explained by bridging neighboring micelles by complexation, because Pd complexes generally connect two olefin groups.[17,18] When the Zeise salt or K_2PtCl_4 are used as the metal source, complexation does not result in precipitation. Presumably, these Pt complexes are mainly intramolecular.[17,18] Electron microscopy reveals for such a sample after interaction with Pt compound a network of wormlike micelles (Figure 5a).

This morphology was also used for casting of mesoporous silica, where again templating was performed with the nonreduced sample. After calcination, TEM and WAXS revealed well-defined Pt nanoparticles of about 4 nm in size located on the border of the pores (Figure 5b). The formation of Pt particles in microporous silica derived from PB-*b*-PEO-III was also performed in a different way. Again a nonreduced sample was employed as the template, but then microporous silica was reduced with H_2 in the mixture of water/ethanol (9/1) at 50 °C for 1 h before calcination. As a result, the color of the powder turned from yellow to gray. The WAXS data of MS−Pt-4b (before calcination) show broad signals, which cannot be evaluated quantitatively, while after calcination the sample MS−Pt-4a contains very tiny particles of 2 nm size (1.57 wt % Pt). In this case, essentially all of the nanoparticles are located in big pores formed by the PB cores.

In summary, variation of the PB-*b*-PEO block copolymers of different block lengths and composition enables

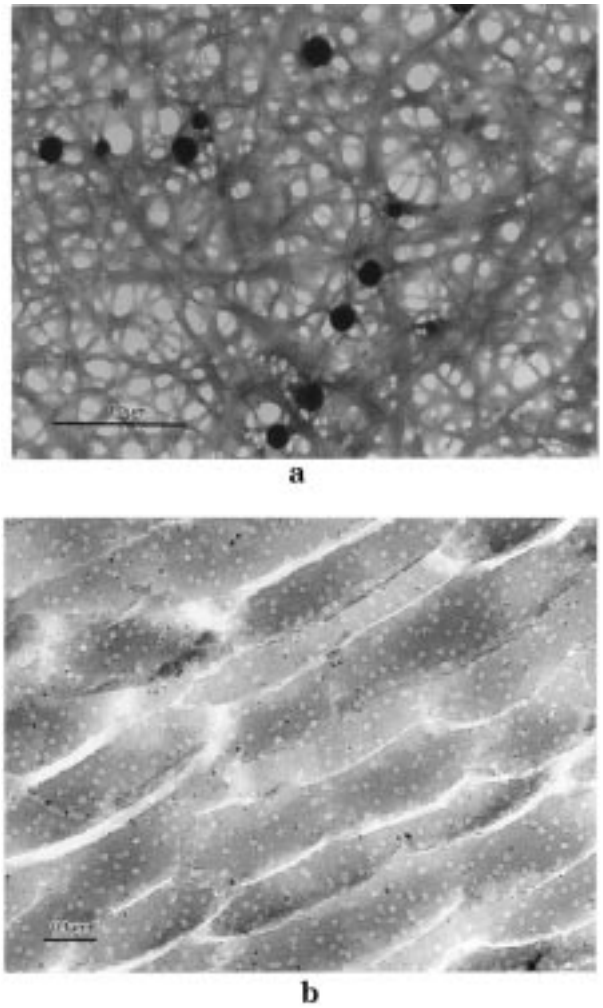

Figure 5. (a) TEM of PB-*b*-PEO-III + Zeise salt. (b) TEM of microporous silica MS−Pt-3a derived from PB-*b*-PEO-III + K_2PtCl_4, when calcination was performed on an unreduced sample.

the adjustment of the pore size and pore structure of microporous silica and therefore the simultaneous size control of metal nanoparticles. By varying metal compounds or the way of metal particle formation and treatment, we are able to affect the metal particle size and particle size distribution. This approach seems to be general and can be used for amphiphilic block copolymers, which form dense micelles in water and have a core which is able to coordinate with metal compounds.

Acknowledgment. We are thankful for the financial support provided by the Max Planck Society and the Volkswagen Foundation. L.B. also thanks the Russian Foundation for Basic Research (Grant 98-03-33372) for support of this research.

CM980762H